Quantum field theory simulations with Rydberg atoms

Yannick Meurice

The University of Iowa
with Sergio Cantu (QuEra), James Corona (U. Iowa), Fangli Liu (QuERA), Kenny Heitritter (qbraid), Steve Mrenna (Fermilab), Shan-Wen Tsai (UCR), Shengtao Wang (QuERA), and Jin Zhang (ChongQing U.)
QuLAT collaboration
yannick-meurice@uiowa.edu
Supported by the Department of Energy under Award Number DOE DE-SC0019139 and DE-SC0010113

YITP 9/15/2023

Students and postdocs

Research Group at U. Iowa

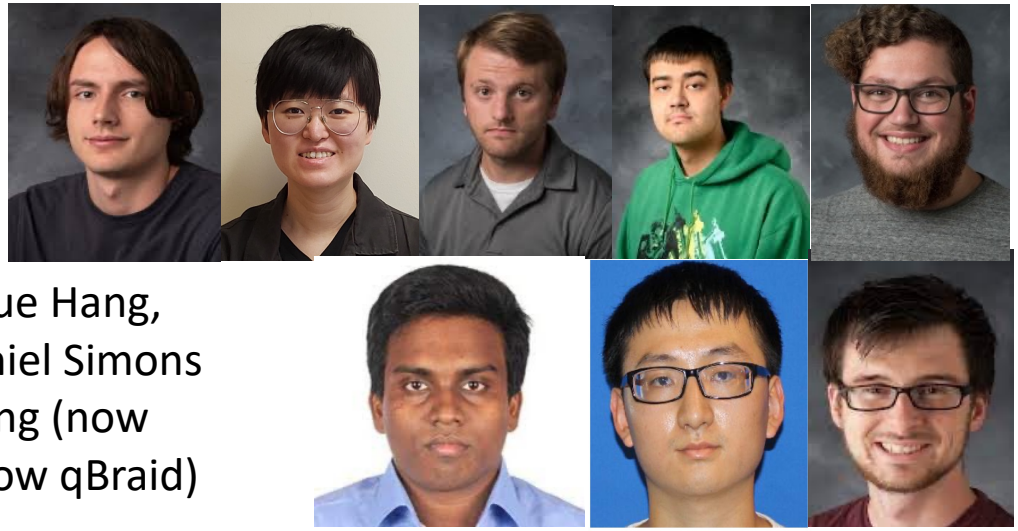

- Grad. students: James Corona, Zheyue Hang, Michael Hite, Robert Maxton, and Daniel Simons
- PostDocs: M. Asaduzzaman, Jin Zhang (now Chongqing U.) and Kenny Heitritter (now qBraid)

High-Energy Physics:

- B-meson decays with lattice gauge theory
- Composite models for the Higgs boson
- Applications of the Renormalization Group
- Tensor formulations of lattice field theory
- Machine learning in MC simulations

Quantum computing:

- Real-time evolution of field theory models
- Quantum computing (IBMQ and trapped ions)
- Quantum simulations (Rydberg atoms, QuEra)

Former graduate students

Yuzhi Liu (Ph. D. 2013): postdocs at U. Colorado Boulder and Indiana U.; Software engineer at Google
Haiyuan Zou (Ph. D. 2014): postdocs at Pittsburgh U. and T. D. Lee Center; Assistant Prof. at East China Normal Un.
J. Unmuth-Yockey (Ph. D. 2017): postdocs at Syracuse U. and Fermilab.
Z. Gelzer (Ph. D. 2017): postdoc at U. Illinois UC.
D. Floor (Ph. D. 2018), Software engineer in Brazil.
S. Foreman (Ph. D. 2019): postdoc at Argonne Nat. Lab.
E. Gustafson (Ph. D. 2021): postdoc at Fermilab
D. Simons (Ph. D. 2023)

QuLAT Collaboration

https://qulat.sites.uiowa.edu/

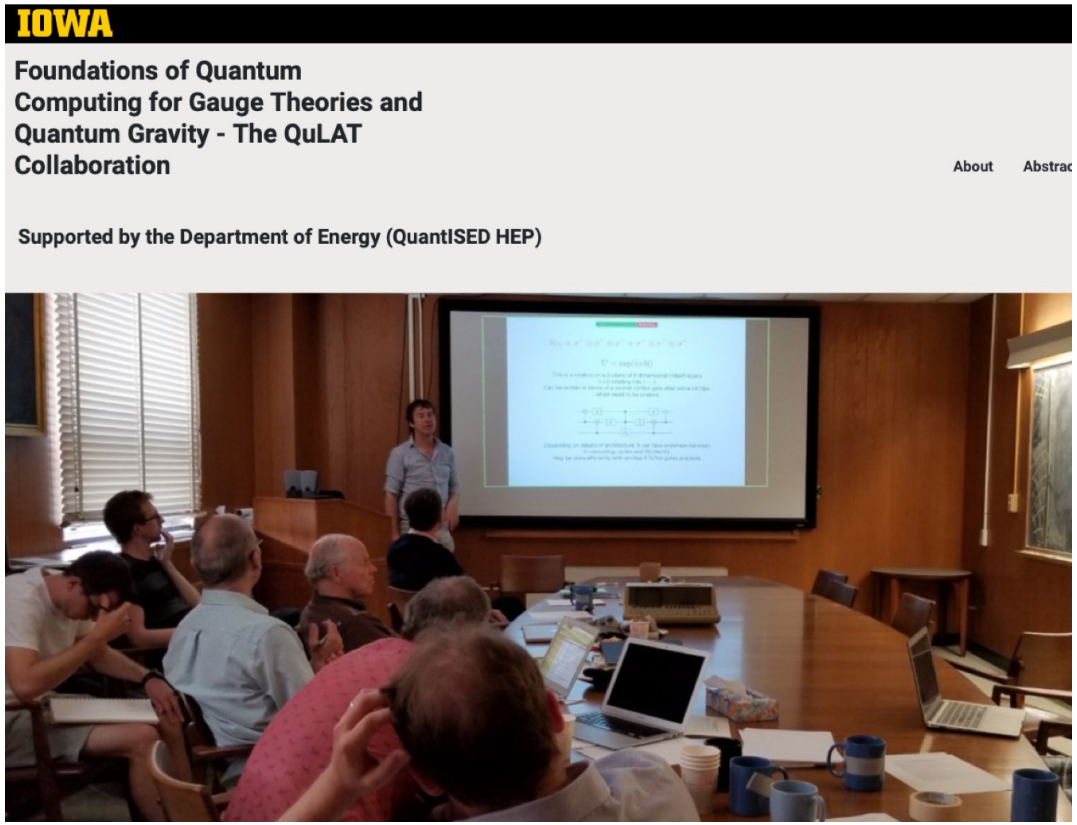

Goals of the collaboration

Quantum computers are expected to exceed the capacity of classical computers and to revolutionize several aspects of computation especially for the simulation of quantum systems. We develop new methods for using quantum computers to study aspects of the evolution of strongly interacting particles in collisions, the quantum behavior of gravitational systems and the emergence of space-time which are beyond the reach of classical computing. Our goal is to design the building blocks of universal quantum computers relevant for these problems and develop algorithms which scale reasonably with the size of the system.

Principal Investigators

Alexei Bazavov, Michigan State University
David Berenstein, University of Cal. Santa Barbara
Richard Brower, Boston University
Simon Catterall, Syracuse University
Xi Dong, UCSB (consultant)
Stephen Jordan, University of Maryland/Microsoft
Seth Lloyd, MIT (consultant)
Yannick Meurice, University of Iowa (Spokesperson)

Contents

- Quantum computing for High Energy Physics
- Hybrid hadronization in event generators?
- Tensor Network methods for lattice gauge theory
- Toy model: the compact Abelian Higgs Model (Scalar QED)
- Model building (literally!) with Arrays of Rydberg atoms
- Matching the target model with the simulator (or vice-versa!)
- Effective theory for the simulator
- Practical examples and work with QuEra
- Phase diagram of the simulator
- Towards an hybrid event generator (QuPYTH), with K. Heitritter and S. Mrenna, arxiv:2212.02476
- Quantum Ising model on two dimensional anti-de Sitter space with Muhammad Asaduzzaman, Simon Catterall, and Goksu Can Toga, arxiv 2309.04383

Big picture

- Monte Carlo methods applied to Lattice Quantum Chromodynamics (QCD) at Euclidean time have been very successful at calculating the static properties of strongly interacting particles (masses, form factors, ...).
- These methods are not effective to deal with the real-time evolution of strongly interacting particles in collisions (jet physics, fragmentation, ...) or their behavior at finite density.
- Quantum computers or quantum simulation experiments offer new directions to deal with these issues.
- We need to start with simple models, use existing resources and build up towards Quantum Chromodynamics following the Euclidean time roadmap (the “Kogut sequence").
- We need to use actual Noisy Intermediate Scale Quantum (NISQ) machines and demonstrate progress for methods (economical truncations, large Trotter steps ...) and hardware.

Ab-initio jet physics : a realistic long term goal?

- Pythia, Herwig, and other jet simulation models encapsulate perturbative QCD results at short distance and empirical models to describe the large distance behavior.
- Crucial for the interpretation of collider physics experiments.
- Could we replace the large distance part by ab-initio lattice QCD calculations?

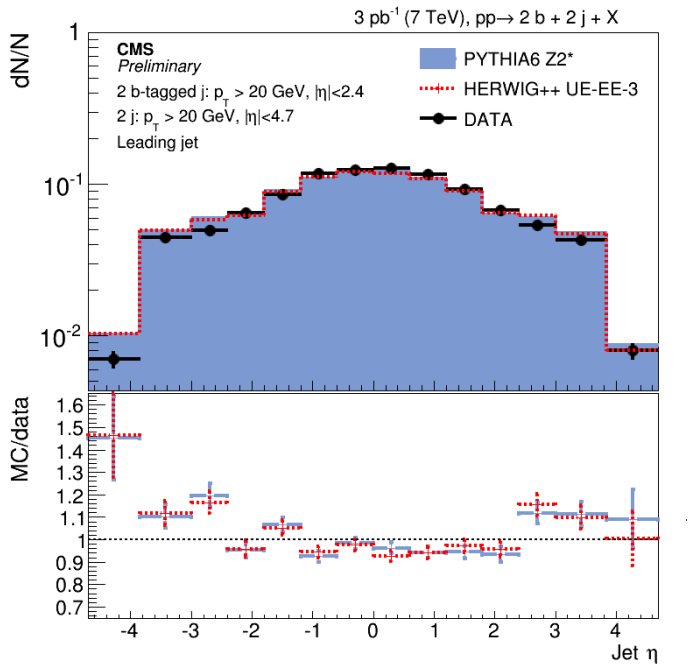

Figure: $pp \to b\bar{b}$ + jets, from CMS.

Hybrid hadronization in event generators?

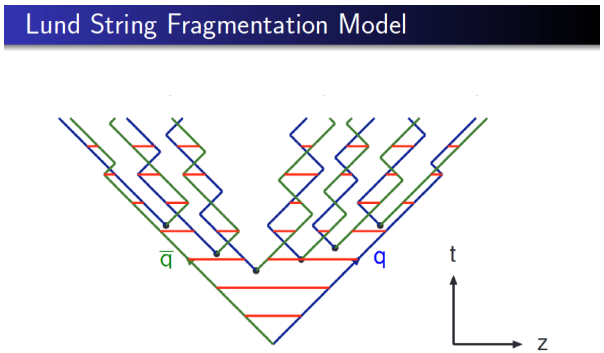

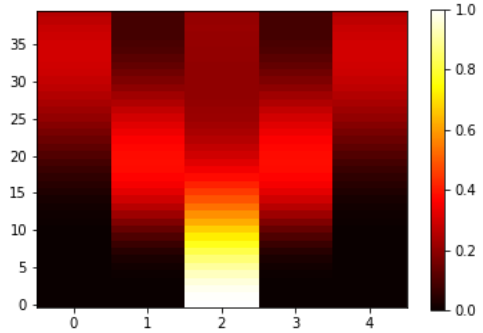

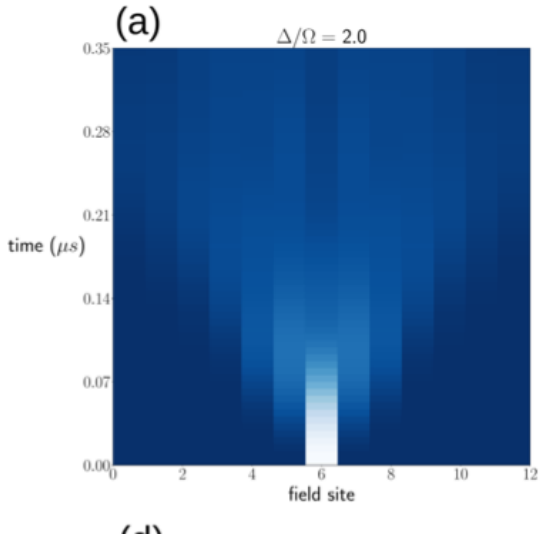

Hadronization of a particle-antiparticle pair with the Lund model/Pythia (left), the Abelian Higgs model in 1+1 dimensions (middle), and a Rydberg atom simulator for this model (right). You may think about the Abelian Higgs model as a toy “ab-initio" lattice model.

Lessons from lattice gauge theory

We need to start with simple models

Figure: Mike Creutz's calculator used for a Z_2 gauge theory on a 3^4 lattice (circa 1979).

Clear goals and good fundamentals (and some help from Moore's law) led to major accomplishments in HEP and NP.

A first step: the quantum ising model in 1+1 dim.

The Hilbert space: N_s qubits for N_s sites

Basic Trotter steps: PRD 99 09453

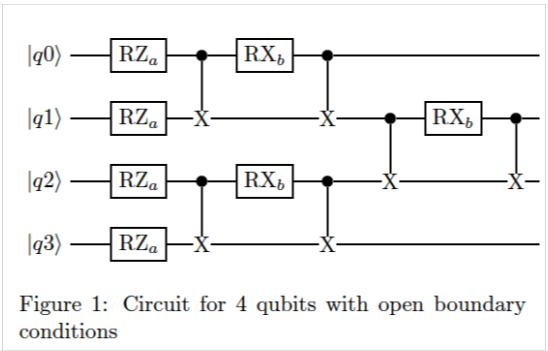

Figure 1: Circuit for 4 qubits with open boundary conditions

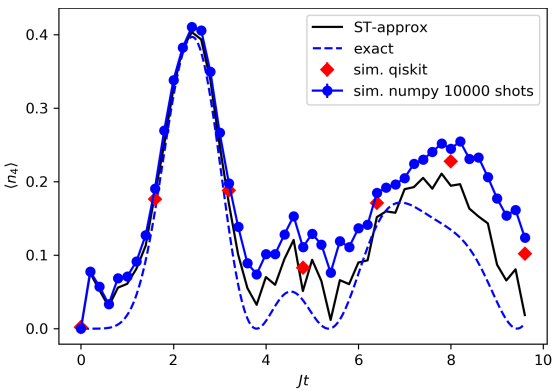

IBMQ Mitigations
JQST 6 045020

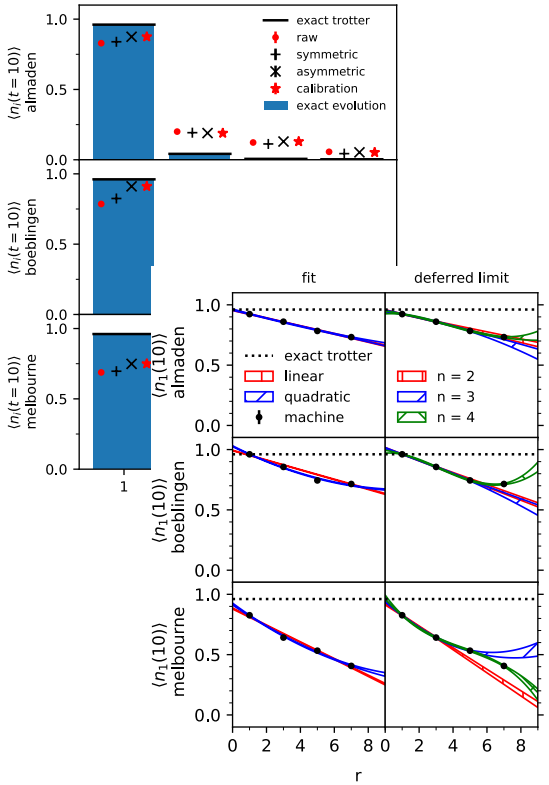

Phase shifts
PRD 104 054507

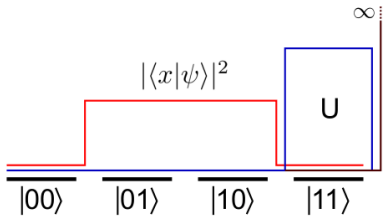

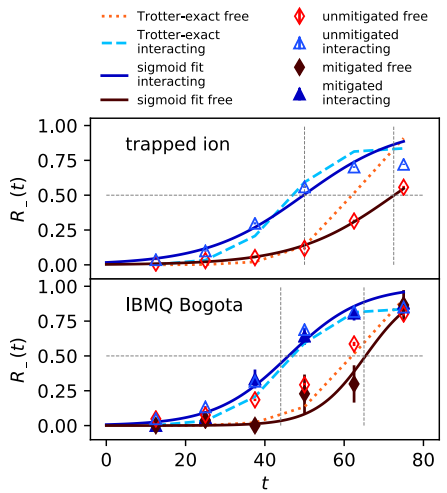

Discretization of problems classically intractable

Quantum computing (QC) requires a complete discretization

- Discretization of space: lattice gauge theory formulation
- Discretization of field integration: tensor methods

Important ideas of the tensor reformulation:

- Character expansions (such as Fourier series): partition function and averages become discrete sums of contracted tensors.
- The “hard" integrals are done exactly and field integrations provide Kronecker deltas that encode the symmetries.
- For continuous field variables, the sums are infinite, but truncations to finite sums do not break symmetries. Y. M., PRD 100, 014506 (2019) and PRD 102 014506 (2020).
- Tensors are the local building blocks of a new formulation

Refs: Y. M., R. Sakai, and J. Unmuth-Yockey, Tensor field theory with applications to quantum computing, arXiv:2010.06539; Reviews of Modern Physics Rev. Mod. Phys. 94, 025005.
Y. M., QFT: a quantum computation approach, IoP book.

Introductions to Tensor Field Theory

REVIEWS OF MODERN PHYSICS, VOLUME 94, APRIL–JUNE 2022

Tensor lattice field theory for renormalization and quantum computing

Yannick Meurice
Department of Physics and Astronomy, The University of Iowa, Iowa City, Iowa 52242, USA

Ryo Sakai
Department of Physics and Astronomy, The University of Iowa, Iowa City, Iowa 52242, USA and Department of Physics, Syracuse University, Syracuse, New York 13244, USA

Judah Unmuth-Yockey
Department of Physics, Syracuse University, Syracuse, New York 13244, USA and Fermi National Accelerator Laboratory, Batavia, Illinois 60510, USA

(published 26 May 2022)

The successes and limitations of statistical sampling for a sequence of models studied in the context of lattice QCD are discussed and the need for new methods to deal with finite-density and real-time evolution is emphasized. It is shown that these lattice models can be reformulated using tensorial methods where the field integrations in the path-integral formalism are replaced by discrete sums. These formulations involve various types of duality and provide exact coarse-graining formulas that can be combined with truncations to obtain practical implementations of the Wilson renormalization group program. Tensor reformulations are naturally discrete and provide manageable transfer matrices. Truncations with the time continuum limit are combined, and Hamiltonians suitable for performing quantum simulation experiments, for instance, using cold atoms, or to be programmed on existing quantum computers, are derived. Recent progress concerning the tensor field theory treatment of noncompact scalar models, supersymmetric models, economical four-dimensional algorithms, noise-robust enforcement of Gauss's law, symmetry preserving truncations, and topological considerations are reviewed. Connections with other tensor network approaches are also discussed.

DOI: 10.1103/RevModPhys.94.025005

CONTENTS

IOP Publishing | Bookstore

Home | Quantum Field Theory

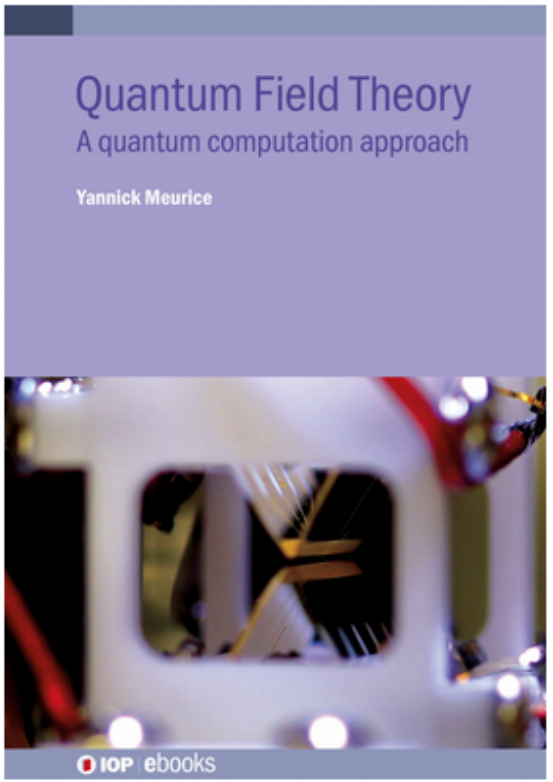

Interdisciplinary effort

SVD and TN methods developed in condensed matter (T. Nishino, X-G. Wen, M. Levin, Tao Xiang, ...). Character expansions used in strong coupling expansions (C. Itzykson, ...). Cutting edge effort in Japan: S. Akiyama, D. Kadoh, Y. Kuramashi, R. Sakai, S. Takeda, Y. Yoshimura, ...

INT WORKSHOP INT-21R-1C

Tensor Networks in Many Body and Quantum Field Theory

April 3, 2023 - April 7, 2023

ORGANIZERS

Simon Catterall
Syracuse University
smcatterall@gmail.com

Glen Evenbly
Georgia Institute of Technology
glen.evenbly@gmail.com

Yannick Meurice
University of Iowa
annick-meurice@uiowa.edu

Alessandro Roggero
University of Washington
roggero@uw.edu

DIVERSITY COORDINATOR

Alessandra Roggero
University of Washington
roggero@uw.edu

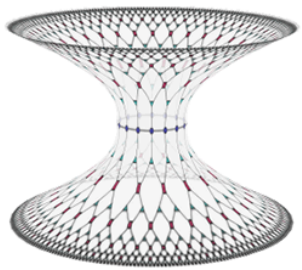

APPLICATION FORM - FOR FULL CONSIDERATION, APPLY BY NOVEMBER 27, 2022

OVERVIEW

Note to applicants: This is an in-person workshop. There is no virtual/online option for this event at this time. Please be aware that all participants must show proof of vaccination against COVID-19 upon arrival to the INT.

Disclaimer: Please also be aware that due to ongoing concerns regarding the COVID-19 pandemic, the workshop may be cancelled.

Tensor network methods are rapidly developing and evolving in many areas of

TLFT: From compact to discrete (O(2) example)

$$Z_{O(2)} = \prod_x \int_{-\pi}^{\pi} \frac{d\varphi_x}{2\pi} e^{\beta \sum_{x,\mu} \cos(\varphi_{x+\hat{\mu}} - \varphi_x)} = \mathrm{Tr} \prod_x T^{(x)}_{n_{x-\hat{1},1}, n_{x,1}, \ldots, n_{x,D}}.$$

$$e^{\beta \cos(\varphi_{x+\hat{\mu}} - \varphi_x)} = \sum_{n_{x,\mu}=-\infty}^{\infty} e^{i n_{x,\mu} \varphi_{x+\hat{\mu}}} I_{n_{x,\mu}}(\beta) e^{-i n_{x,\mu} \varphi_x}.$$

$$\text{Tensor}: \; T^{(x)}_{n_{x-\hat{1},1}, n_{x,1}, \ldots, n_{x-\hat{D},D}, n_{x,D}} = \sqrt{I_{n_{x-\hat{1},1}} I_{n_{x,1}}, \ldots, I_{n_{x-\hat{D},D}} I_{n_{x,D}}} \times \delta_{n_{x,\mathrm{out}}, n_{x,\mathrm{in}}},$$

$$\prod_x \int_{-\pi}^{\pi} d\varphi_x \Longrightarrow \sum_{\{n\}}$$

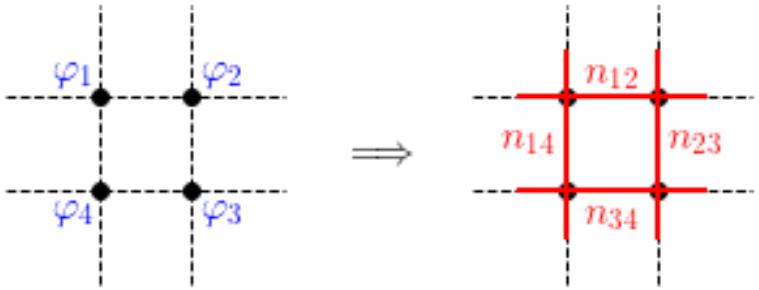

The gauged version is the Abelian Higgs model.

Compact Abelian Higgs Model (CAHM)

The lattice compact Abelian Higgs model is a non-perturbative regularized formulation of scalar quantum electrodynamics (scalar electrons-positrons + photons with compact fields).

$$Z_{CAHM} = \prod_x \int_{-\pi}^{\pi} \frac{d\varphi_x}{2\pi} \prod_{x,\mu} \int_{-\pi}^{\pi} \frac{dA_{x,\mu}}{2\pi} e^{-S_{gauge}-S_{matter}},$$

$$S_{gauge} = \beta_{plaquette} \sum_{x,\mu<\nu} (1 - \cos(A_{x,\mu} + A_{x+\hat{\mu},\nu} - A_{x+\hat{\nu},\mu} - A_{x,\nu})),$$

$$S_{matter} = \beta_{link} \sum_{x,\mu} (1 - \cos(\varphi_{x+\hat{\mu}} - \varphi_x + A_{x,\mu})).$$

- local invariance: $\varphi'_x = \varphi_x + \alpha_x$ and $A'_{x,\mu} = A_{x,\mu} - (\alpha_{x+\hat{\mu}} - \alpha_x)$.
- φ is the Nambu-Goldstone mode of the original model. The Brout-Englert-Higgs mode is decoupled (heavy).

Assembly of the A (links, blue) and B (plaquette, red) tensors for $D = 2$ (Figures by Ryo Sakai)

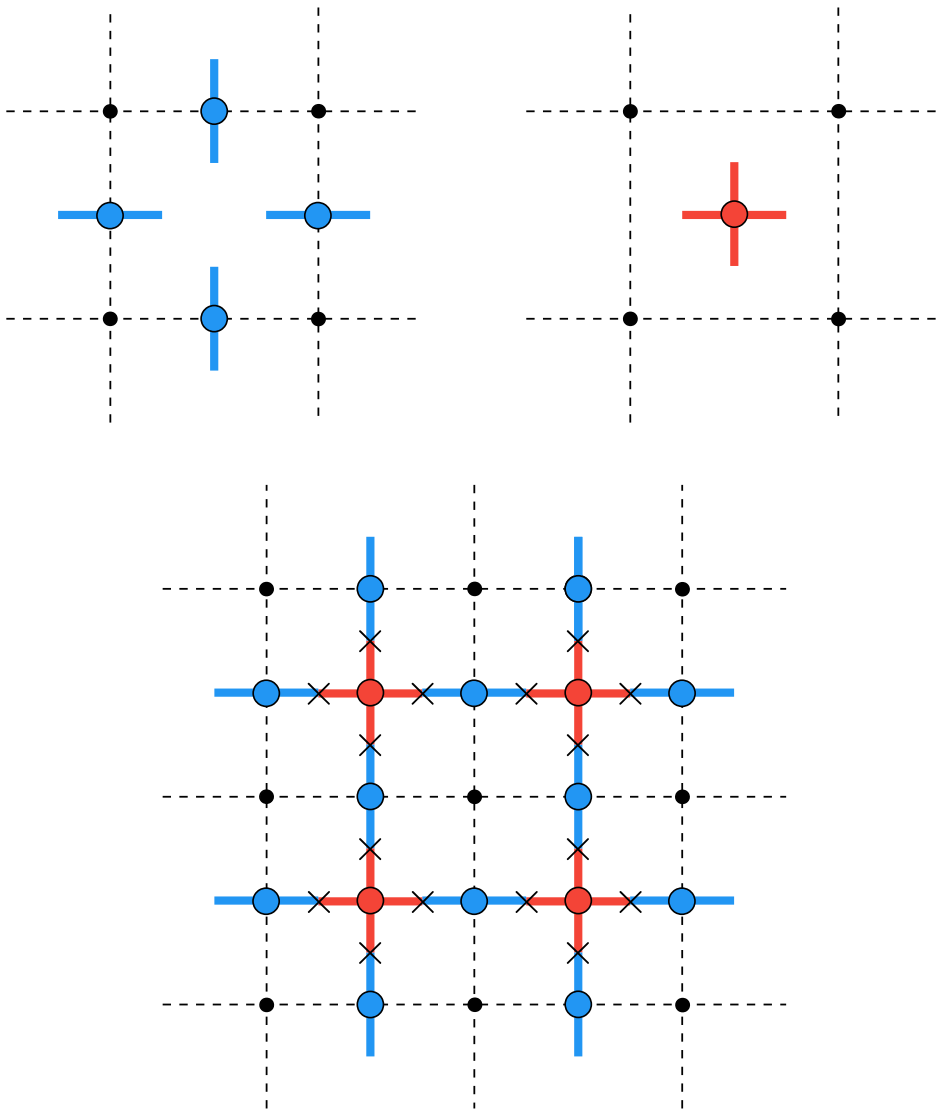

Assembly of the A (links, blue) and B (plaquette, red) tensors for $D = 3$ (Figures by Ryo Sakai)

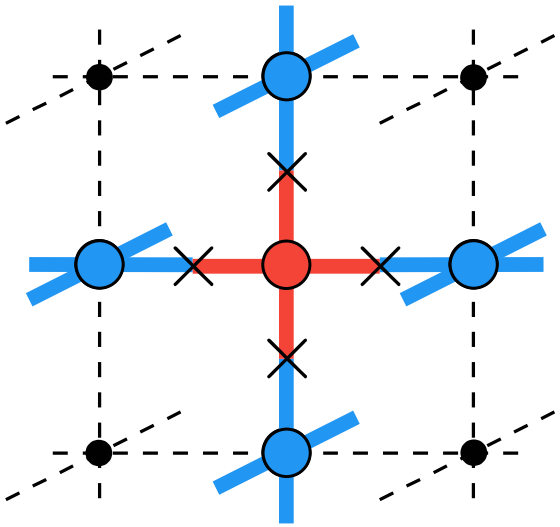

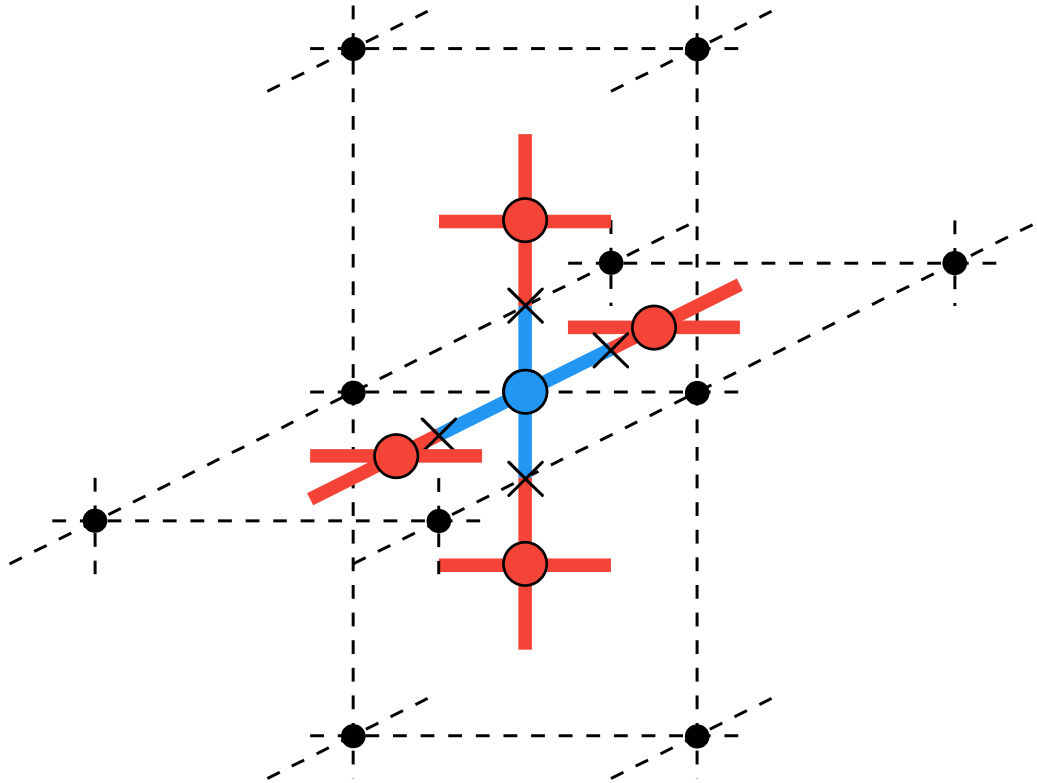

Transfer matrix and Gauss's law with NISQ machines

PHYSICAL REVIEW D **102,** 014506 (2020)

Discrete aspects of continuous symmetries in the tensorial formulation of Abelian gauge theories

Yannick Meurice*

Department of Physics and Astronomy, The University of Iowa, 514 Van Allen Hall, Iowa City, Iowa 52242, USA

(Received 7 April 2020; accepted 30 June 2020; published 14 July 2020)

We show that standard identities and theorems for lattice models with $U(1)$ symmetry get reexpressed discretely in the tensorial formulation of these models. We also explain the geometrical analogy between the continuous lattice equations of motion and the discrete selection rules of the tensors. We further construct a gauge-invariant transfer matrix in arbitrary dimensions, show the equivalence with its gauge-fixed version in a maximal temporal gauge, and explain how a discrete Gauss's law is always enforced. Moreover, we propose a noise-robust way to implement Gauss's law in arbitrary dimensions, and we reformulate Noether's theorem for global, local, continuous, or discrete Abelian symmetries: for each given symmetry, there is one corresponding tensor redundancy. We discuss semiclassical approximations for classical solutions with periodic boundary conditions in two solvable cases, and we show the correspondence of their weak coupling limit with the tensor formulation after Poisson summation. Finally, we briefly discuss connections with other approaches and implications for quantum computing.

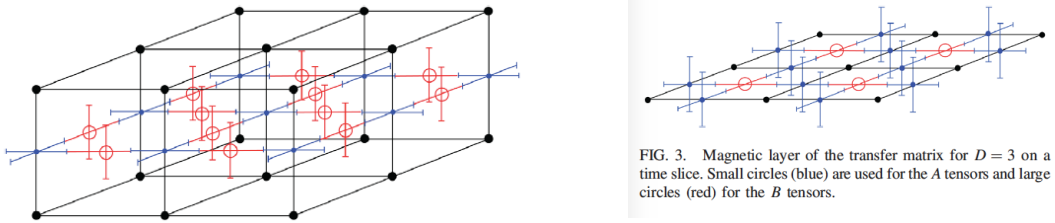

FIG. 3. Magnetic layer of the transfer matrix for $D = 3$ on a time slice. Small circles (blue) are used for the A tensors and large circles (red) for the B tensors.

For introduction to Tensor Lattice Field Theory (TLFT) see Y. M., R. Sakai, and J. Unmuth-Yockey, Rev. Mod. Phys. 94, 025005;
Y. M., QFT: a quantum computation approach, IoP book.

Tensors as computational building blocks

- The partition functions are traces of product of tensors
- Observables can be calculated by introducing “impure" tensors
- Tensors are local
- They contain all the information about the model, its dimension and symmetries (universality)
- Most lattice models have a tensor reformulations
- They can be coarse-grained exactly
- RG procedure require truncations (this is the hard part)
- The space of tensors is easier to handle than the space of interactions
- Smooth connection between Lagrangian (path integral) and Hamiltonian using transfer matrix.
- Tensors can be used to build quantum circuits

FAQ: Do truncations break global symmetries? No (Y.M. arXiv 1903.01918, PRD 100, 014506)

- Truncations of the tensorial sums are necessary, but do they break the symmetries of the model?
- Non-linear O(2) sigma model and its gauged version (the compact Abelian Higgs model), on a D-dimensional cubic lattice: truncations are compatible with symmetry identities.
- This selection rule is due to the quantum number selection rules at the sites and is independent of the particular values taken by the tensors (e. g. 0, discrete form of a vector calculus theorem).
- Extends to global $O(3)$ symmetries (you need to keep all the m's for a given ℓ, related to Wigner-Eckart)
- The universal properties of these models can be reproduced with highly simplified formulations desirable for implementations with quantum computers or for quantum simulations experiments.

Reformulation of Noether's theorem

- Redundant selection rules are in one-to-one correspondence with irrelevant integrations.
- We can skip the integrations that produce redundant selection rules and replace these integrated fields by arbitrary values. This is exactly what gauge-fixing does.
- The redundancy argument extends to discrete $\mathbb{Z}_q$ subgroups of $U(1)$ where the divergenceless condition is expressed modulo q
- Noether's theorem can be expressed in the tensor formulation context as: for each symmetry, there is a corresponding tensor redundancy. This applies to global, local, continuous and discrete Abelian symmetries.

CAHM: Hamiltonian and Hilbert space in 1+1 dim.

The continuous-time limit yields the Hamiltonian

$$H = \frac{U}{2}\sum_{i=1}^{N_s}(L_i^z)^2 + \frac{Y}{2}\sum_i (L_{i+1}^z - L_i^z)^2 - X\sum_{i=1}^{N_s} U_i^x$$

with $U^x \equiv \frac{1}{2}(U^+ + U^-)$ and $L^z|m\rangle = m|m\rangle$ and $U^\pm|m\rangle = |m \pm 1\rangle$.

- m is a discrete electric field quantum number ($-\infty < m < +\infty$)
- In practice, we need to apply truncations: $U^\pm|\pm m_{max}\rangle = 0$.
- We focus on the spin-1 truncation ($m = \pm 1, 0$ and $U^x = L^x/\sqrt{2}$.)
- U-term: electric field energy.
- Y-term: matter charges (determined by Gauss's law)
- X-term: currents inducing temporal changes in the electric field.

Target simulations (E-field, spin-1, 5 sites)

$$H = \frac{U}{2}\sum_{i=1}^{N_s}\left(L_i^z\right)^2 + \frac{Y}{2}\sum_i (L_{i+1}^z - L_i^z)^2 - X\sum_{i=1}^{N_s} U_i^x$$

Initial state: particle-antiparticle (connected by an electric field +1)

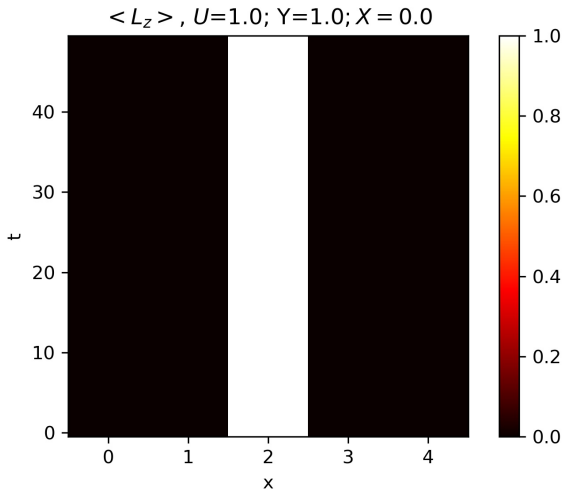

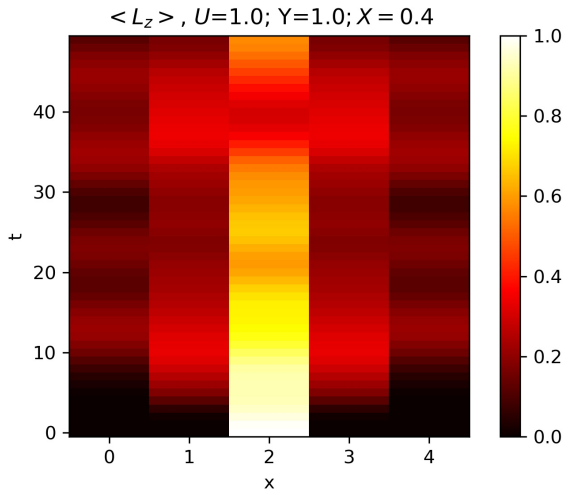

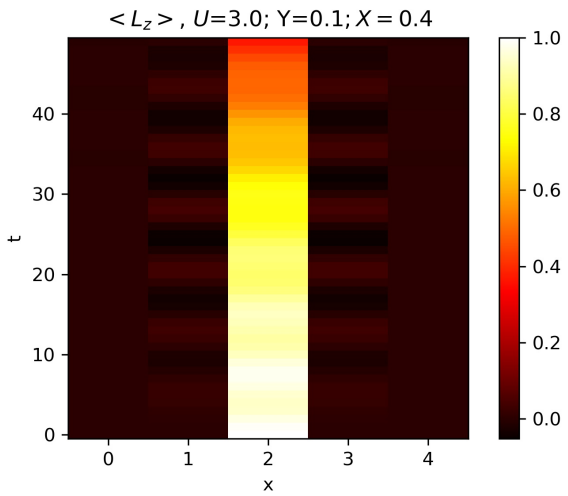

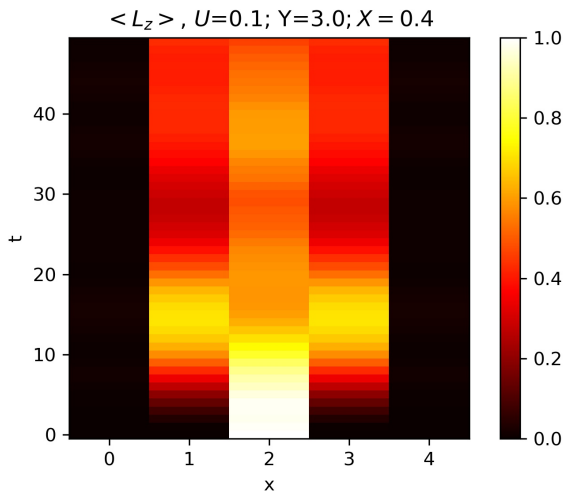

Configurable Arrays of Rydberg Atoms (CARA)

- One can adapt (Y.M., PRD 104) the optical lattice construction (J. Zhang et al. PRL 121) using ^{87}Rb atoms separated by controllable (but not too small) distances, coupled to the excited Rydberg state $|r\rangle$ with a detuning Δ.
- The ground state is denoted $|g\rangle$ and the two possible states $|g\rangle$ and $|r\rangle$ can be seen as a qubit. $n|g\rangle = 0,\ n|r\rangle = |r\rangle$.
- The (effective) Hamiltonian reads

$$H = \frac{\Omega}{2}\sum_i (|g_i\rangle\langle r_i| + |r_i\rangle\langle g_i|) - \Delta\sum_i n_i + \sum_{i<j} V_{ij} n_i n_j,$$

with

$$V_{ij} = \Omega R_b^6 / r_{ij}^6,$$

for a distance r_{ij} between the atoms labelled as i and j. Note: when $r = R_b$, $V = \Omega$.

- This repulsive interaction prevents two atoms close enough to each other to be both in the $|r\rangle$ state. This is the so-called blockade mechanism.

One site spin-1 with 2 and 3 atoms (Y.M. PRD 104)

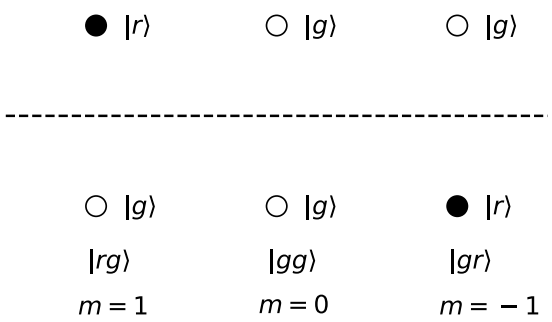

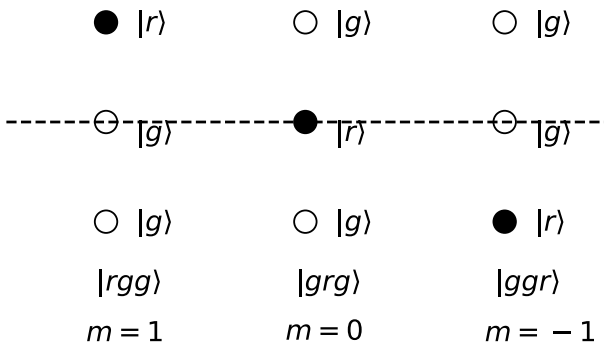

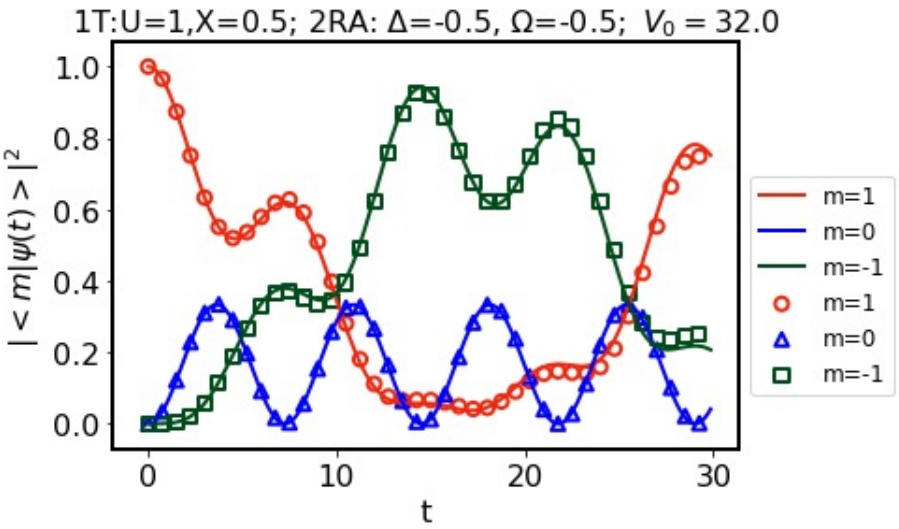

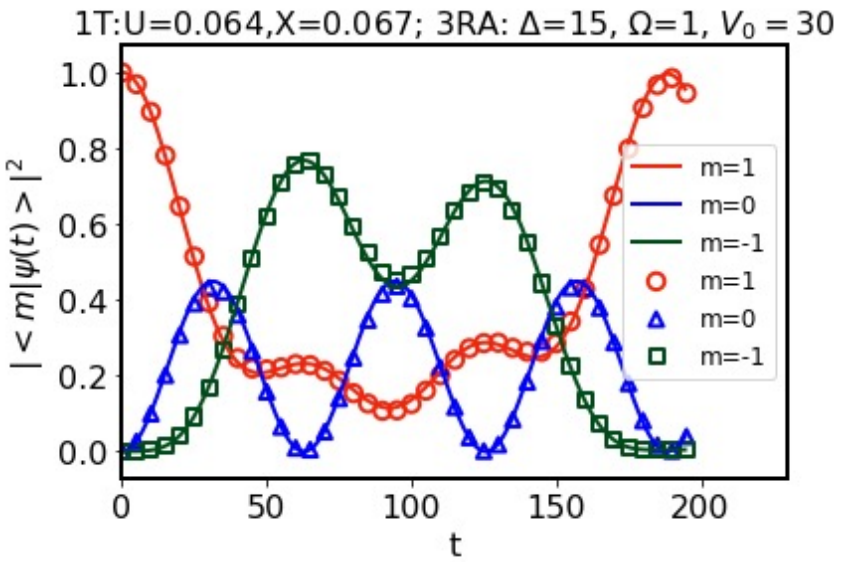

Solid line: target, Symbols: simulator

Exact matching vs. study of continuum limit

- 1 site, 2 atoms: exact up to $|rr\rangle$ transitions (when $\Omega = 0$, can be implemented by setting $\Delta = -U/2$ and $\Omega = -X$
- 2 sites, 4 atoms: when $X = \Omega = 0$ reads $\Delta = -U/2 - \frac{Y}{2},\ V_1 = Y,\ V_2 = -Y$. No solution with current technology (homogeneous setup).

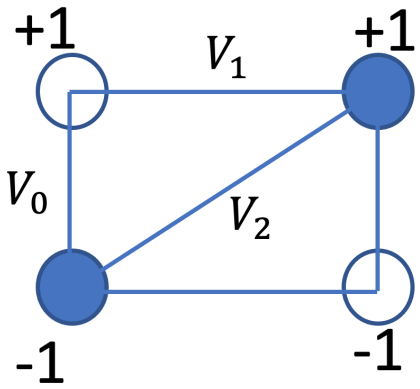

- 1 site, 3 atoms: it's complicated! (ideally: inhomogeneous Δ to split $m = 0$ and $m = \pm 1$, otherwise use degenerate perturbation theory as a guide, James Corona's work in progress).

A better approach may be to study all the continuum limits (where correlation lengths become large) that can be obtained with the simulator.

QuEra

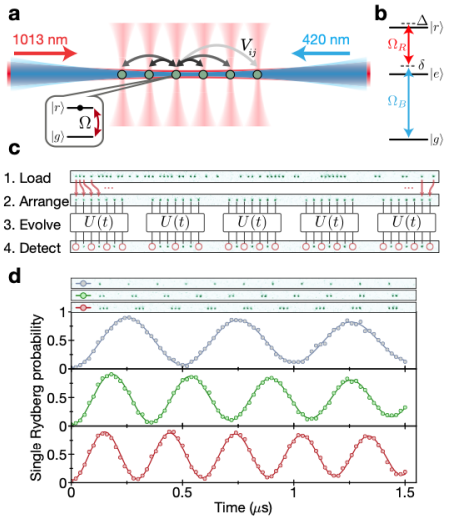
a
1013 nm
420 nm
V_{ij}
$|r\rangle$
$|g\rangle$
Ω
b
Δ
$|r\rangle$
Ω_R
δ
$|e\rangle$
Ω_B
$|g\rangle$
c
1. Load
2. Arrange
3. Evolve
4. Detect
$U(t)$
d
Single Rydberg probability
Time (μs)

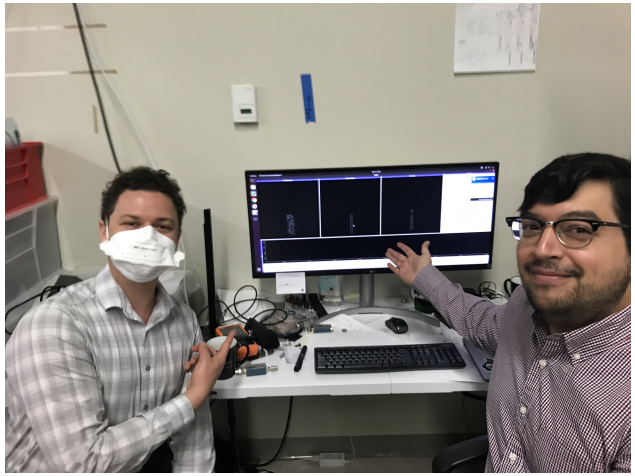


QuEra

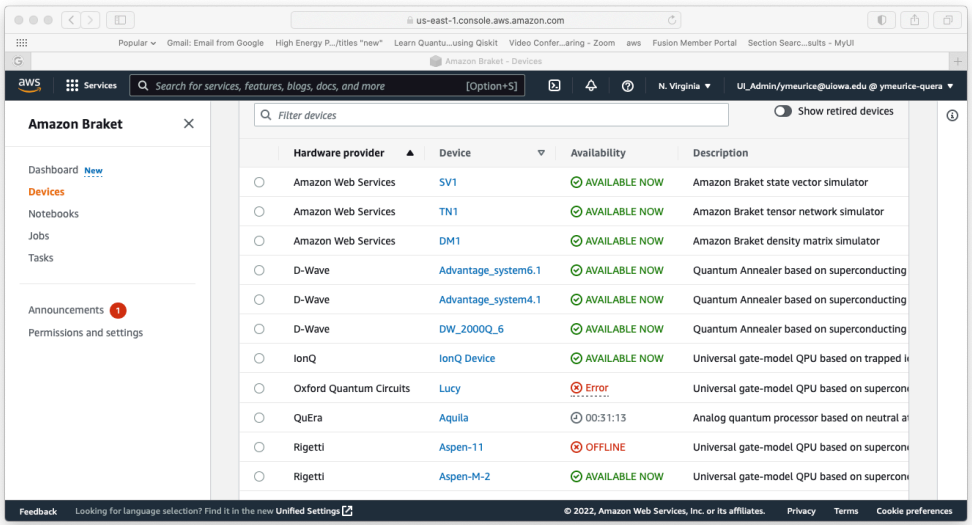
us-east-1.console.aws.amazon.com
aws
Services
Search for services, features, blogs, docs, and more
[Option+S]
N. Virginia
UI_Admin/ymeurice@uiowa.edu @ ymeurice-quera
Amazon Braket
Dashboard New
Devices
Notebooks
Jobs
Tasks
Announcements
Permissions and settings
Filter devices
Show retired devices
Hardware provider
Device
Availability
Description
Amazon Web Services SV1 AVAILABLE NOW Amazon Braket state vector simulator
Amazon Web Services TN1 AVAILABLE NOW Amazon Braket tensor network simulator
Amazon Web Services DM1 AVAILABLE NOW Amazon Braket density matrix simulator
D-Wave Advantage_system6.1 AVAILABLE NOW Quantum Annealer based on superconducting
D-Wave Advantage_system4.1 AVAILABLE NOW Quantum Annealer based on superconducting
D-Wave DW_2000Q_6 AVAILABLE NOW Quantum Annealer based on superconducting
IonQ IonQ Device AVAILABLE NOW Universal gate-model QPU based on trapped
Oxford Quantum Circuits Lucy Error Universal gate-model QPU based on superco
QuEra Aquila 00:31:13 Analog quantum processor based on neutral a
Rigetti Aspen-11 OFFLINE Universal gate-model QPU based on superco
Rigetti Aspen-M-2 AVAILABLE NOW Universal gate-model QPU based on superco
Feedback
Looking for language selection? Find it in the new Unified Settings
© 2022, Amazon Web Services, Inc. or its affiliates.
Privacy
Terms
Cookie preferences

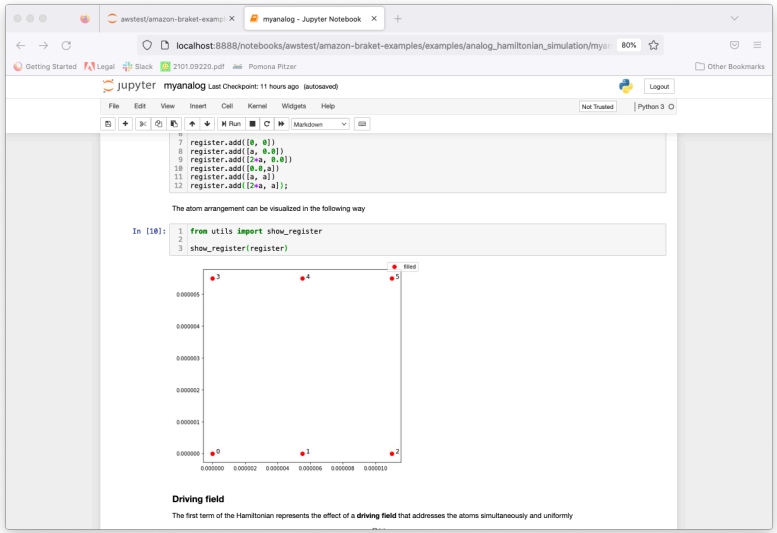
myanalog - Jupyter Notebook
localhost:8888/notebooks/awstest/amazon-braket-examples/examples/analog_hamiltonian_simulation/mya
jupyter myanalog Last Checkpoint: 11 hours ago (autosaved)
register.add([0, 0])
register.add([a, 0.0])
register.add([2*a, 0.0])
register.add([0.0,a])
register.add([a, a])
register.add([2*a, a]);
The atom arrangement can be visualized in the following way
In [10]:
from utils import show_register
show_register(register)
Driving field
The first term of the Hamiltonian represents the effect of a driving field that addresses the atoms simultaneously and uniformly

10 atoms (5 sites) with QuEra and H_{eff}.

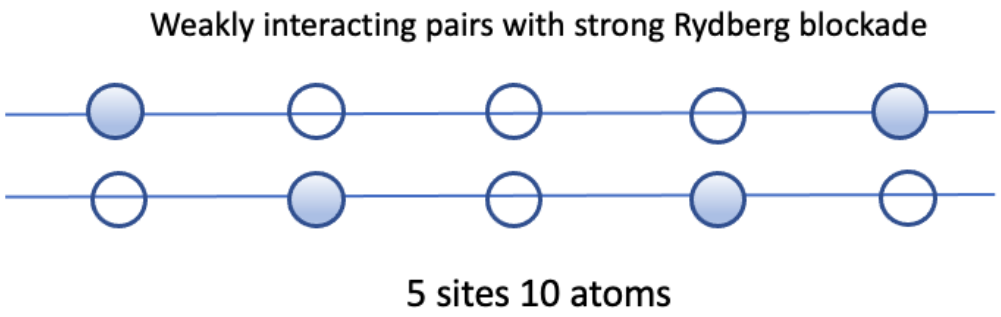


```
In [11]:
register = AtomArrangement()
H = Hamiltonian()

ahs_program = AnalogHamiltonianSimulation(
        hamiltonian=H,
        register=register
    )
for nn in range(nsites):
        register.add([nn*aax, 0])
        register.add([nn*aax, aay])
show_register(register)
```

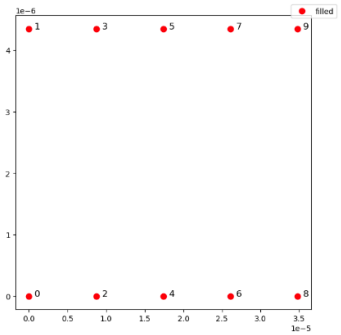

Values of $< L_z^2 >$ for five sites (10 atoms) starting in the $|ggggggggg\rangle$ state, $\Omega = 4\pi MHz$, $\Delta = 2\Omega$, for 50 steps of 10^{-8}s, $a_x = 1R_b \simeq 8.7\mu m$; $a_y = 0.5R_b$ so $|rr\rangle$ at that site are unlikely. Left: exact diagonalization. Middle: QuEra (local simulator). Right: Effective Hamiltonian.

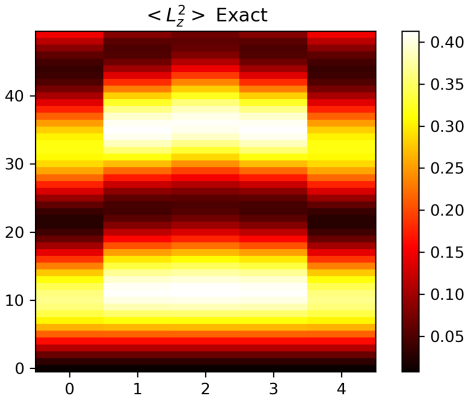

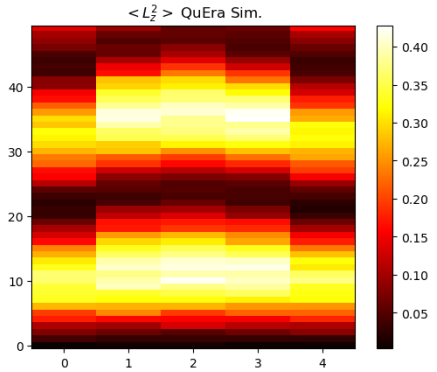

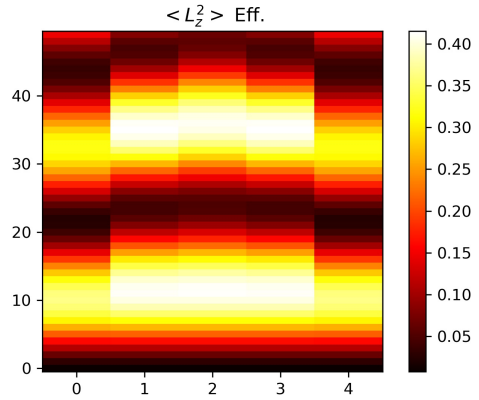

Effective Hamiltonian (with J. Zhang and S.-W. Tsai)

The basic spin relation is $L_i^z = n_{i,2} - n_{i,1}$ for atoms 1 and 2 at a site.
$\left(L_i^z\right)^2 \simeq n_{i,2} + n_{i,1}$ if we ignore $|rr\rangle$.
This implies $n_{i,2(1)} \simeq \left[\left(L_i^z\right)^2 \pm L_i^z\right]/2$.
Plugging into the simulator Hamiltonian we get the effective Hamiltonian

$$\begin{aligned}\hat{H}_{\rm 2LR}^{\rm eff} &= -\Delta \sum_{i=1}^{N_s} (L_i^z)^2 + \sum_k \left(\frac{V_1^{(k)} - V_2^{(k)}}{2} \sum_{i=1}^{N_s-1} L_i^z L_{i+k}^z \right. \\ &\left. + \frac{V_1^{(k)} + V_2^{(k)}}{2} \sum_{i=1}^{N_s-1} (L_i^z)^2 \left(L_{i+k}^z\right)^2 \right) \\ &+ \frac{\Omega}{2} \sum_{i=1}^{N_s} \left(\hat{U}_i^+ + \hat{U}_i^-\right).\end{aligned}$$

If the distance between the sites is of order of 1.0 R_b or more we can neglect the NNN intereactions (which is done in the following).

Exact diagonalization, QuEra and H_{eff}.

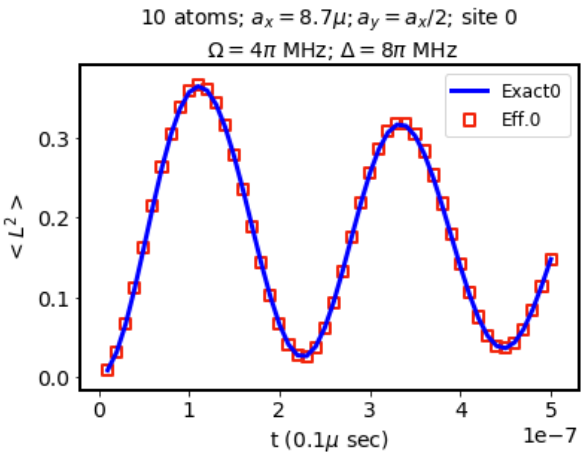

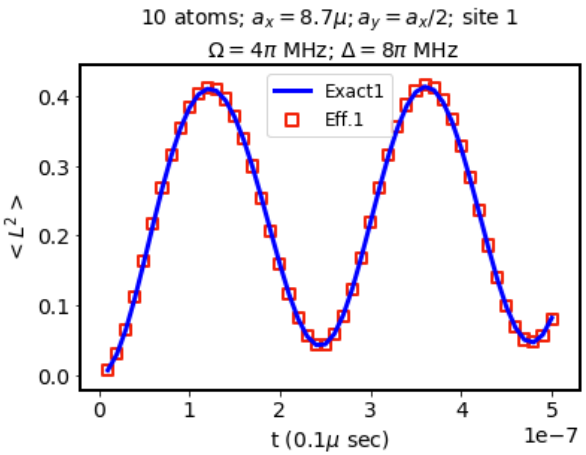

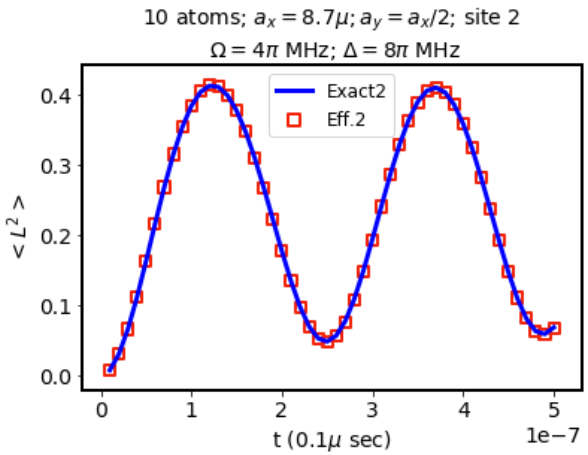

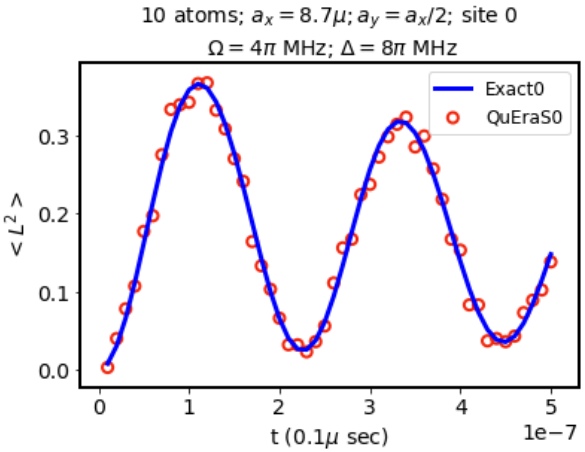

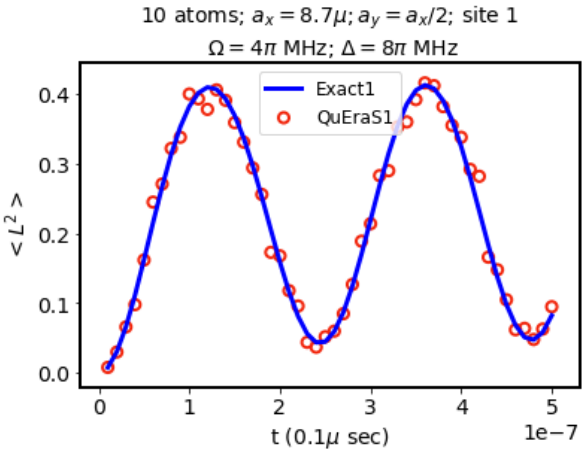

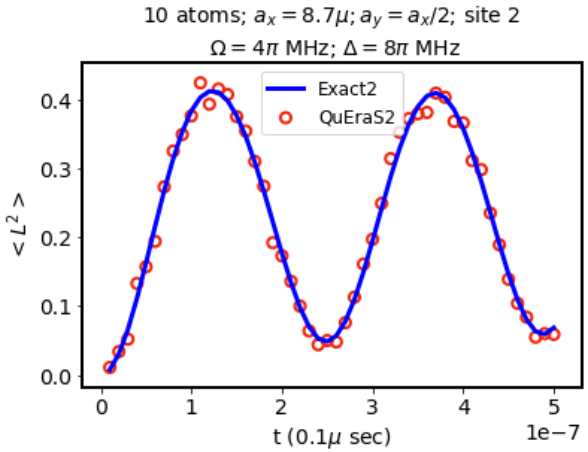

Comparison between $H_{eff.}$ and H_{CAHM}

$$H_{CAHM} = \frac{U}{2}\sum_{i=1}^{N_s}\left(L_i^z\right)^2 - Y\sum_{i=1}^{N_s-1}L_{i+1}^z L_i^z - X\sum_{i=1}^{N_s}U_i^x$$

$$H_{eff.} = -\Delta\sum_{i=1}^{N_s}(L_i^z)^2 + \frac{V_1-V_2}{2}\sum_{i=1}^{N_s-1}L_i^z L_{i+1}^z + \Omega\sum_{i=1}^{N_s}U_i^x + H_{quartic}$$

$$H_{quartic} = \frac{V_1+V_2}{2}\sum_{i=1}^{N_s-1}\left(L_i^z\right)^2\left(L_{i+1}^z\right)^2.$$

Matching

- $\Delta = -U/2$ (sign matters!)
- The coefficient for $L_i^z L_{i+1}^z$ is positive ($V_1 > V_2$) for the simulator (repulsive/antiferromagnetic) but the CAHM has ferromagnetic interactions. This can be remedied by redefining the observable $L_{2i+1}^z \to -L_{2i+1}^z$ (staggered)
- After staggered redefinition, we need $V_1 = -V_2 = Y > 0$ but $V_2 > 0$
- $\Omega = -X$ (sign does not matter)

Everything agrees with two-rung results (YM, PRD104)

Effect of new quartic term (Jin Zhang)

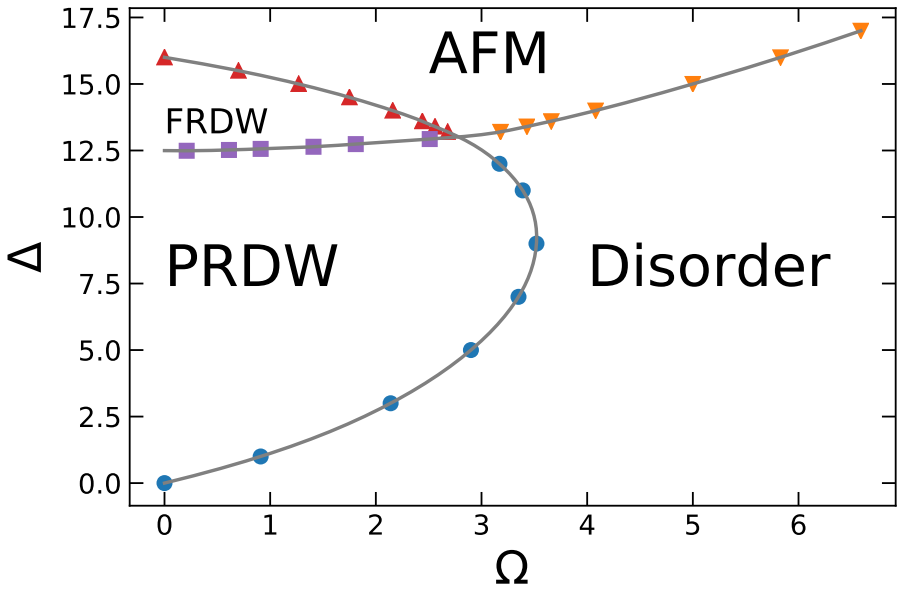

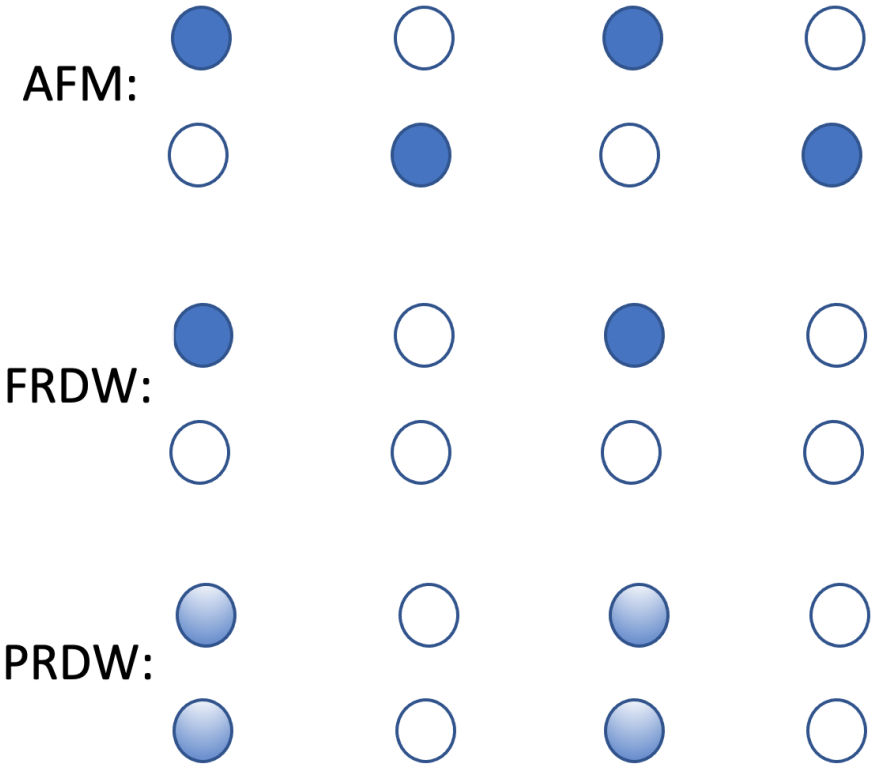

Figure: Ground-state phase diagram for the effective Hamiltonian of the two-leg Rydberg ladder. Here $L = 512$, $V_0 = 1000$, $\rho = dy/dx = 0.5$. The PRDW phase is disordered in even or odd sites, and the FRDW phase is FM in even or odd sites.

Phase diagram for a two-leg ladder.

With Sergio Cantu (QuEra), Fangli Liu (QuERA), Shan-Wen Tsai (UCR), Shengtao Wang (QuERA), Jin Zhang (ChongQing U.)

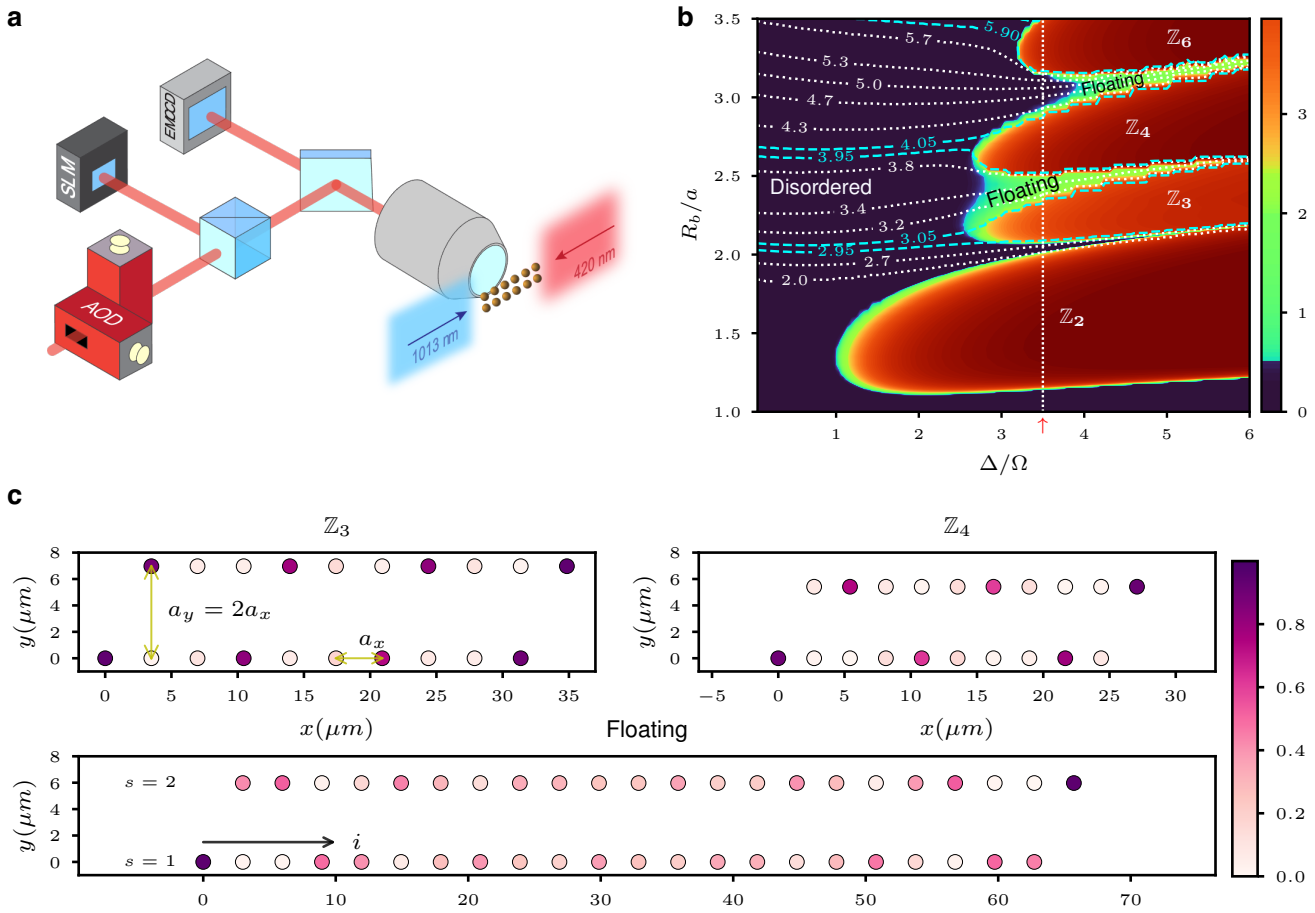

Experimental $< m_i m_j >$ for two-leg ladder

First row: for i and j; second row: versus $i - j$; third row: Fourier Tr.

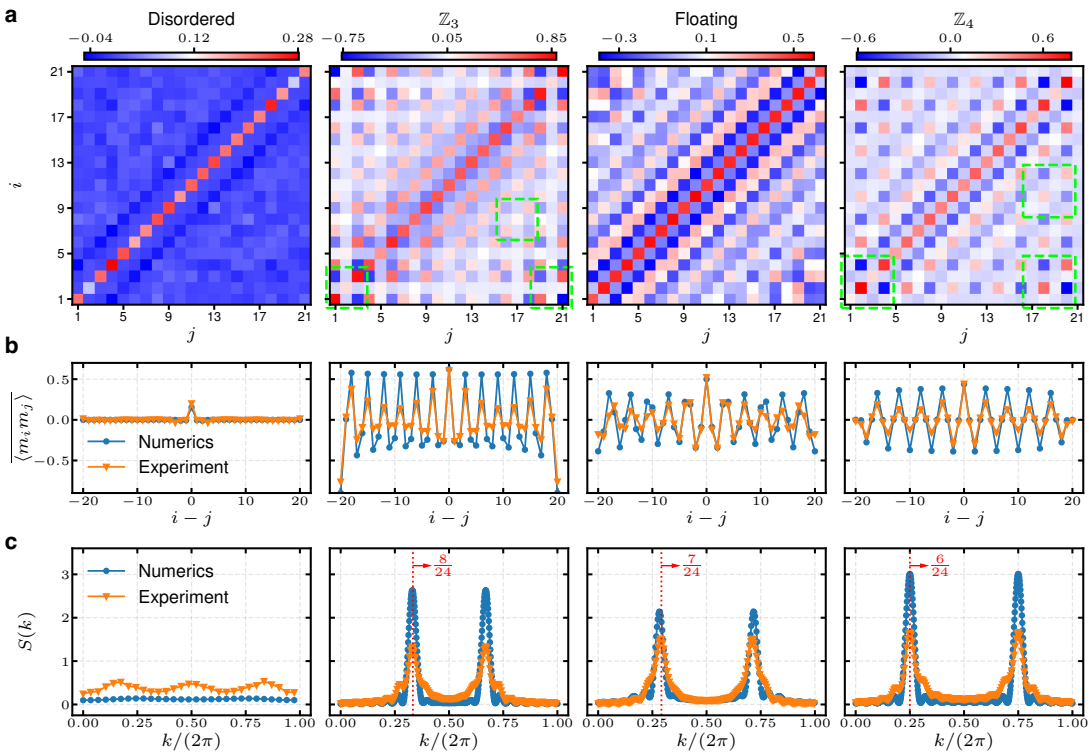

Experimental and Numerical Fourier transforms

The floating phase is characterized by a continuous dependence in the lattice spacing (at infinite volume!).

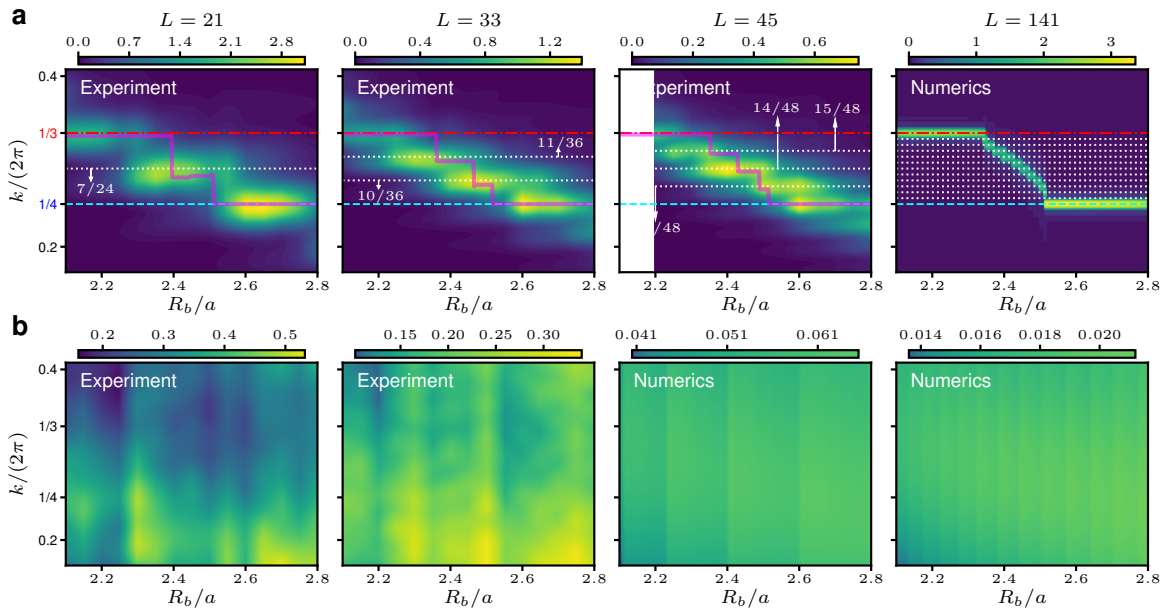

Figure: **The structure factor for different system sizes. a**, The structure factor as a function of R_b/a is measured along the cut $\Delta/\Omega = 3.5$ for $L = 21, 33, 45$. The magenta curves are peak positions from numerical results. The results for $L = 141$ is from numerics. **b**, The structure factor is measured along the cut $\Delta/\Omega = 0$ in the disordered phase.

Hadron Multiplicity (graph by K. Heitritter, 2212.02476)

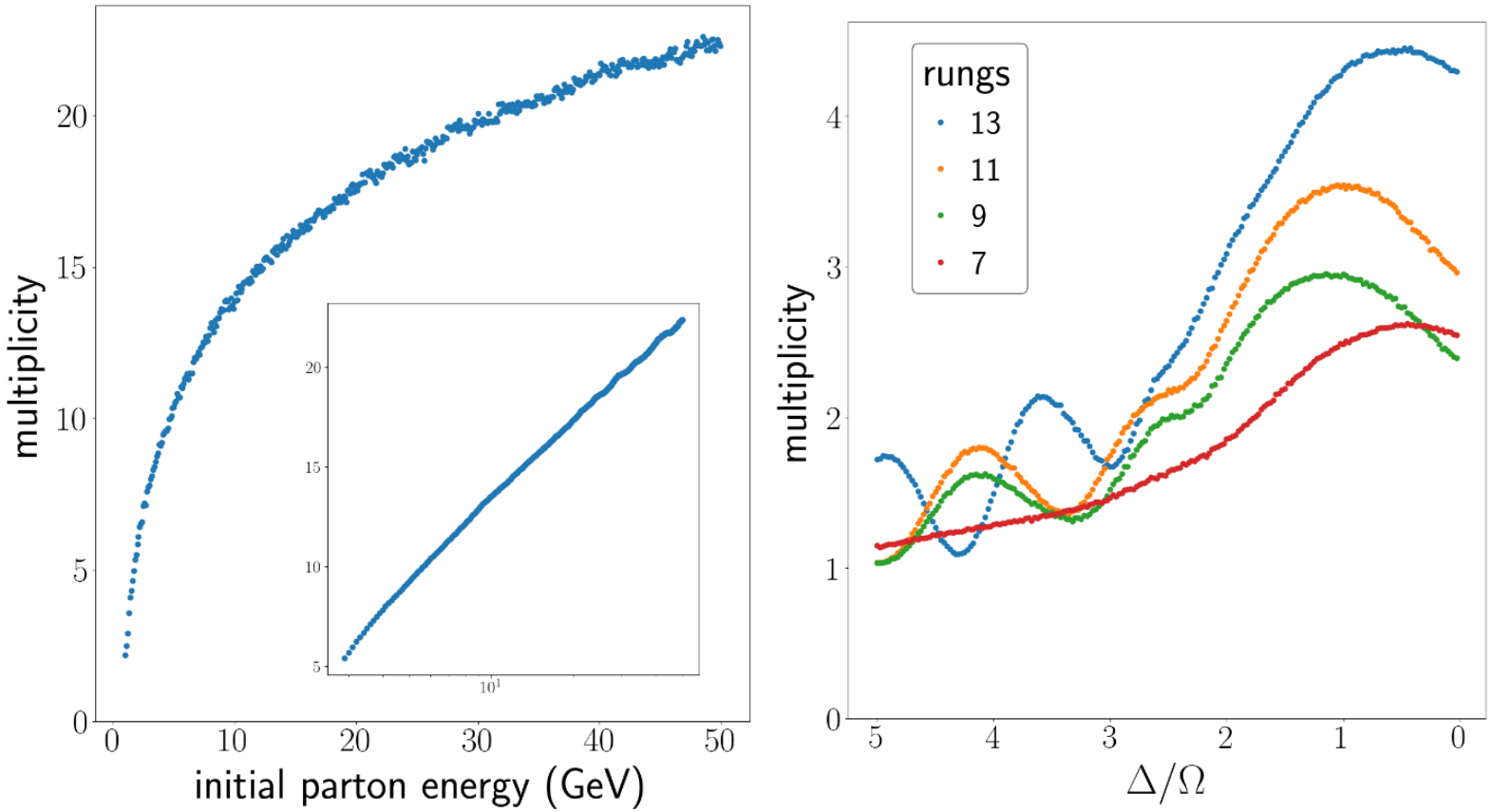

Figure: Left: Hadron multiplicity predictions with default pythia hadronization from an initial $u\bar{u}$ pair. Right: Simple model hadron multiplicity output of the Rydberg hadronization model for $R_b/a = 2.173$. Δ/Ω plotted in decreasing order. The recently public Rydberg simulator, Aquila, has the ability to investigate ladders with 128 atoms.

Quantum Ising model on two dimensional anti-de Sitter space arxiv 2309.04383.

with Goksu Toga, Simon Catterall, M. Asaduzzaman and Ryo Sakai

$$\hat{H} = \frac{-J}{4} \sum_{<ij>} \frac{\cosh(l_i) + \cosh(l_j)}{2} \sigma_i^z \sigma_j^z + \frac{h}{2} \sum_i \cosh(l_i) \sigma_i^x + \frac{m}{2} \sum_i \cosh(l_i) \sigma_i^z .$$

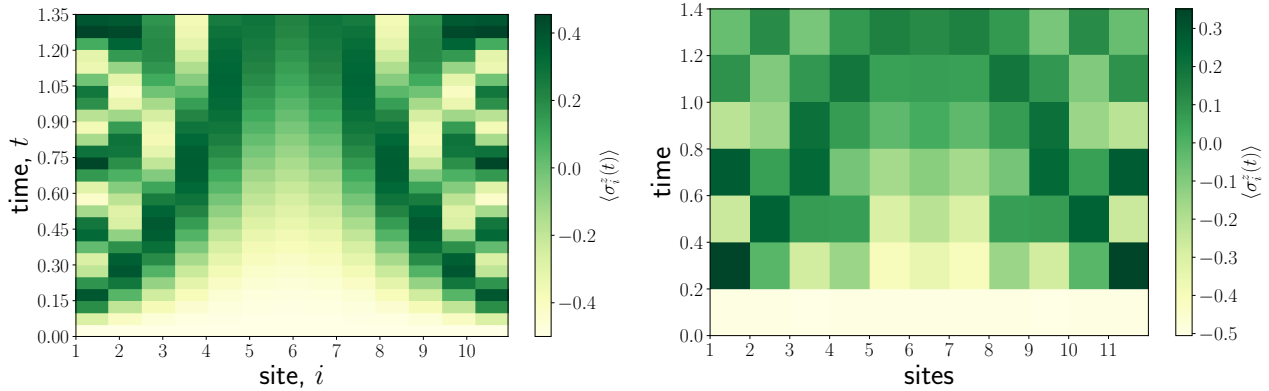

Figure: Trotter evolution with exact diagonalization and using IBM Guadalupe QPU,Parameters: $N = 13$, $J = 2.0$, $h = 1.05$, $l_{\max} = 3.0$. Graphs by Goksu Toga and M. Asaduzzaman.

Out-of-time-ordered-correlator (OTOC)

$$F_{ij}(t) = \langle W_i(t)^\dagger V_j(0)^\dagger W_i(t) V_j(0) \rangle \text{ with } W(t) = \sigma^z(t),\ V = \sigma^z$$

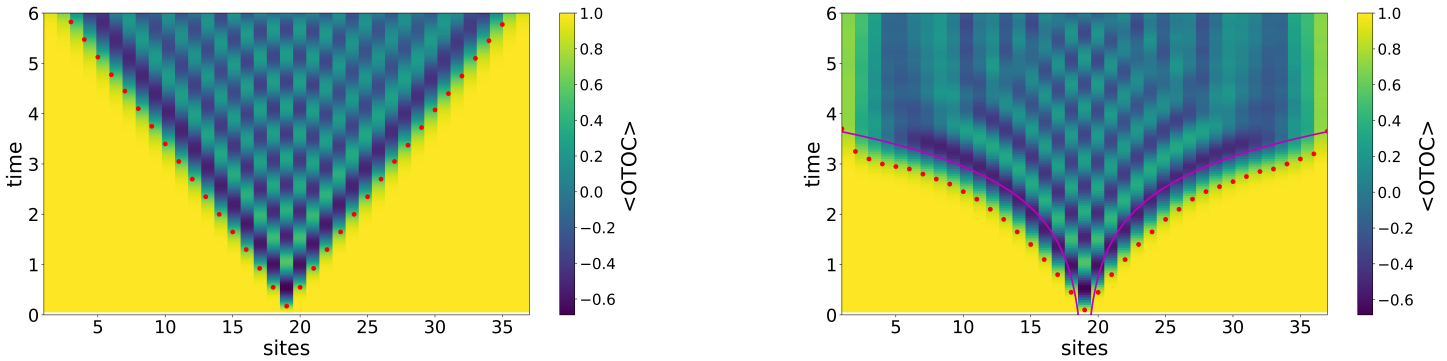

Figure: $W(t)$ is at the center and V_i at different lattice sites i. $J = 6.0$. Left: no curvature. Right: curvature. Graphs by Goksu Toga. See arxiv 2309.04383. Approximate Rydberg implementation under progress. Dey Parijat suggestion: AdS/BCFT by Tadashi Takayanagi arXiv:1105.5165.

What should we explore?

- Matching with gauge theory requires $\Delta < 0$ (cost for producing electric field). The new phases appear when $\Delta > 0$ ($m = \pm 1$ form the degenerate ground state). Could this be used as an environment effect?
- Potential issue with microscopic string breaking -> Staggered structures (cells with two sites) to match other models.
- Go outside the region of validity of H_{eff}.

Other work with Rydberg atoms

- F. M. Surace, P. P. Mazza, G. Giudici, A. Lerose, A. Gambassi, and M. Dalmonte, Phys. Rev. X 10, 021041 (2020).
- A. Celi, B. Vermersch, O. Viyuela, H. Pichler, M. D. Lukin, and P. Zoller, Phys. Rev. X 10, 021057 (2020).
- S. Notarnicola, M. Collura, and S. Montangero, Phys. Rev. Research 2, 013288 (2020).
- Pierre Fromholz, Mikheil Tsitsishvili, Matteo Votto, Marcello Dalmonte, Alexander Nersesyan, Titas Chanda, Phys. Rev. B 106, 155411 (2022)
- Daniel Gonzalez-Cuadra, Torsten V. Zache, Jose Carrasco, Barbara Kraus, Peter Zoller, Phys. Rev. Lett. 129, 160501 (2022)
- For more refs. see: C. Bauer, Z. Davoudi et al., arXiv:2204.03381, PRX Quantum 4 (2023) 2, 027001

Conclusions

- QC/QIS in HEP and NP: big goals with many intermediate steps
- Tensor Lattice Field Theory (TLFT): generic tool to discretize path integral formulations of lattice model with compact variables (truncations preserve symmetries).
- Ladder-shaped Rydberg arrays with two (or three) atoms per site: simulators for the compact Abelian Higgs model.
- Matching between simulator and target model should be understood in the continuum limit (universal behavior).
- Effective Hamiltonians for the simulator: same three types of terms as the target model plus an extra quartic term.
- The two-leg ladder has a very rich phase diagram.
- Implementations with AWS/QuEra (ongoing).
- Progress with hybrid hadronization, evolution in AdS.
- Thanks for listening!
- For questions, email: yannick-meurice@uiowa.edu .

Thanks for listening!

GC=0.3; st=2; $sth = 1.5$; T=1.5

Figure: Isingized version of Emmy Noether